Textures and Microstructures, 1991, Vols 14–18, pp. 769–774
Reprints available from the publisher
Photocopying permitted by license only

TEXTURE DEVELOPMENT DURING GRAIN GROWTH

I. Heckelmann*, X.B. Zhao**, K. Lücke*, G. Abbruzzese***
* Institut für Metallkunde und Metallphysik, RWTH Aachen, FRG
** Zhejiang University, Hangzhou, VR China
*** Centro Sviluppo Materiali, S.P.A. Roma, Italy

INTRODUCTION

Normal or continous grain growth (GG) is defined as continous coarsening of a grain structure during annealing. Burke and Beck [1,2] derived that on the basis of simple energetic considerations the increase of the mean radius $\bar{R}$ is proportional to t^n with t as annealing time and 0.5 as kinetic exponent n. It is well known that the presence of particles and/or preferred orientations in the initial state, e.g. after primary recrystallization, cause deviations from normal GG. Both lead to a change of the kinetics of GG ($n \neq 0.5$) and may result in a marked abnormal GG (secondary recrystallization).

A detailed treatment of GG in the presence of textures was given by Abbruzzese and Lücke (AL-theory) [3,4,5]. They derived a general statistical model taking into account anisotropic grain boundary (GB) energies and mobilities which allows the calculation of the time evolution of the grain size and grain orientation distribution as function of time. In the present paper results of the AL-model will be presented, analytically explained and compared to GG experiments on single phase Al 0.5% Mn and Al 3% Mg alloys.

GRAIN GROWTH EXPERIMENTS IN THE PRESENCE OF TEXTURE

The specimens were cold rolled and subsequently recrystallized. The grain size distributions were determined by linear intercept measurements. The ODF's were calculated from the measured {111}, {200}, {220} and {113} pole figures by the series expansion method. Using the Gauss model analyses[6] a quantitative description in terms of volume fractions of the texture components was obtained. For both alloys after primary recrystallization a strong Cube texture was found. The subsequent GG in both cases lead to a complete change of texture. The kinetics could not be described even approximately by a unique time law with n=0.5.

The Al 0.5% Mn alloy was cold rolled 93%, recrystallized and subsequently annealed at 620°C. Fig.1a shows the mean radius as function of the annealing time in a double logarithmic plot. After short annealing

times there is a period of fast GG with n=2.2 followed by a period of very slow increase of the mean grain size with n=0.2. Fig.1b shows the corresponding volume fractions of the involved texture components and Fig.1c the corresponding {111} pole figures. After primary recrystallization the texture mainly consists of the Cube component, which sharpens after short

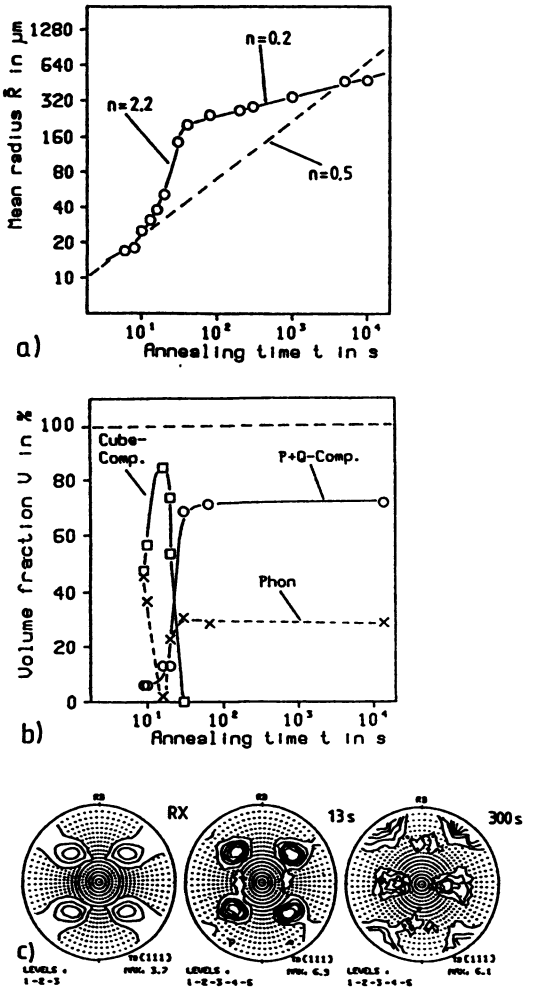

Fig.1: Experimental data as function of annealing time for Al 0.5% Mn; (a) Mean radius; (b) Volume fractions of the Cube, P+Q and random oriented grains; (c) {111} pole figures.

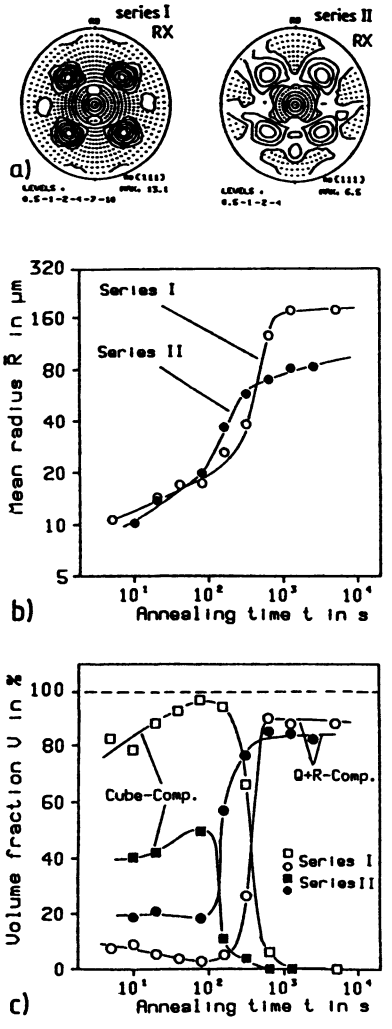

Fig.2: Experimental data as function of annealing time for Al 3% Mg (series I and II). (a) {111} pole figures after primary recrystallization; (b) Mean radius; (c) Volume fractions of the main texture components.

annealing times considerably at the expense of the here also present high fraction of randomly oriented grains (phon). Subsequently, in the period of fast GG, first a texture component denoted as P-component (77°,45°, 0°) and then also the Q-component (55°,0°,0°) whose initial volume fractions were too small to be resolved have grown at the expense of the Cube component until the latter was completedly consumed.

The Al 3% Mg alloy was colled rolled 95%. For primary recrystallization two annealing temperatures were applied: one series of the specimens were annealed for 10 minutes at 300°C (series I) and another series for 0.5 minutes at 450°C (series II). The different annealing temperatures caused different initial textures. This can be seen from the {111} pole figures of Fig.2a where the Cube component at 300°C is much sharper than at 450°C, and from Fig.2c where the initial volume fractions for the Cube orientation differ considerably (40% compared to 80%). All specimens were subsequently annealed for GG at 450°C. Fig.2b shows in a double logarithmic plot the development of the mean radius as function of time for both series. Qualitatively they behave in the same manner: At the beginning the average grain size grows slowly, then a period of fast GG follows which finally passes again into a very slow increase of grain size. But for series I the kinetic curve of the fast growth period is much steeper and results in a grain size which is more than two times higher than for the samples of series II. In both cases the steep increase of grain sizes is again accompanied by a complete transition of texture (Fig.2c). Both series start with a strengthening of the cube component (up to nearly 100% volume fraction for series I), and result in a texture which for series I mainly consists of the Q- and R-component (59°,37°,63°) and for series II only of the Q-component.

THEORETICAL TREATMENT OF GRAIN GROWTH

For 2-dimensional (2D) GG with constant GB energies and mobilities it was shown by von Neumann and Mullins[7] that the growth rate of an individual grain (dA/dt, A is the area of the grain) linearly depends on the number of its sides n. Using the linear relationship between radius R and mean number of sides n (as proved by thorough experiments and by theoretical considerations[8]) the following rate equation can be derived:

$$dR/dt = m\gamma/2\ (1/R_c - 1/R) \qquad \text{with} \quad R_c = \bar{R} \qquad (1)$$

R_c represents a critical radius in a way that grains with $R>R_c$ will grow and with $R<R_c$ will shrink. It is also shown in [8] that the same rate equation (Eq.1) is obtained by a statistical approach considering grains as circles (AL-model). In this model the calculation of the driving force of each grain boundary is based on the superposition of the shrinking pressures between adjacent grains. The rate equation (Eq.1) together with a continuity equation allows the numerical calculation of the time evolution of the grain size distribution during GG.

This statistical treatment can easily be transferred to 3D GG where grains are considered as spheres instead of circles (2D). Here the rate equation reads

$$dR/dt = m\gamma\,(1/R_c - 1/R) \qquad \text{with} \quad R_c = \overline{R^2}/\bar{R} \qquad (2)$$

The treatment of GG in the presence of textures requires to distinguish the energies and mobilities of GBs between differently oriented grains. Then one obtains a rate equation for each orientation which depends not only on R but also on γ and m of the surrounding grains. E.g. for a microstructure with two texture components A and B the simulation of GG requires as input parameters the grain size distribution of both components A and B as well as the energies and mobilities of all GB-types existing in the 2-orientation case, i.e. γ_{AA}, γ_{AB}, γ_{BB}, m_{AA}, m_{AB}, m_{BB}.

GRAIN GROWTH SIMULATION WITH 2 TEXTURE COMPONENTS AND COMPARISION WITH EXPERIMENTS

Two simulations were carried out considering two texture components A and B. As initial state for both simulations a log-normal grain size distribution was chosen but with different initial volume fractions V_A and V_B for the components A and B. For the first simulation V_A was set to 90% (V_B=10%), and for the second simulation V_A=70% (V_B=30%). The energies and mobilities of GBs between grains of the same component are assumed to be equal ($\gamma_{AA}=\gamma_{BB}$, $m_{AA}=m_{BB}$) and small compared to the values of the (large angle) A-B GBs, namely γ_{AB}/γ_{AA}=1.4 and m_{AB}/m_{AA}=5.0. Figs.3a,b show the results of the simulations. The time evolution of the grain size as well as of the texture are qualitatively the same as found experimentally during GG in Al 3% Mg (Figs.2) where also different volume fractions existed in the initial state. At the beginning the majority component A sharpens, and later the minority component B consumes the A-component completely. Also some detailed conformities could be found, e.g. a retardation of the texture change in the case of a sharper initial texture.

For Al 3% Mg (series I) also a quantitative fitting of the simulation to the experimental results was carried out. Here the 1D grain radii had to be transformed into 3D grain radii using the polyeder model[9]. Considering as components C (Cube) and Q+R, the partial grain size distributions (i.e. those separated for the two components) were determined using the etch pit technique. Figs.4a,b show the results. It can be seen that all stages of GG could be described very exactly. As simulation input the initial grain size distributions were given; the normalized values of γ and m were chosen as follows: ($\gamma^{CC}m^{CC} = 3.9\cdot10^{-12}$ m²/s)

$$\begin{vmatrix} \gamma^{C\,C} & \gamma^{C\,Q+R} \\ & \gamma^{Q+R\,Q+R} \end{vmatrix} = \begin{vmatrix} 1.0 & 1.6 \\ & 1.3 \end{vmatrix}; \quad \begin{vmatrix} m^{C\,C} & m^{C\,Q+R} \\ & m^{Q+R\,Q+R} \end{vmatrix} = \begin{vmatrix} 1.0 & 6.0 \\ & 4.0 \end{vmatrix}.$$

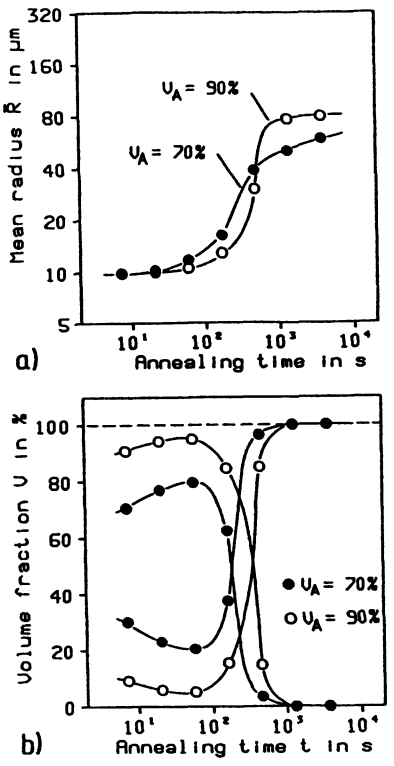

Fig.3: Model calculation data as function of annealing time for initial volume fractions of V_A=70% and of V_A=90%. (a) Mean radius; (b) Volume fractions V_A and V_B.

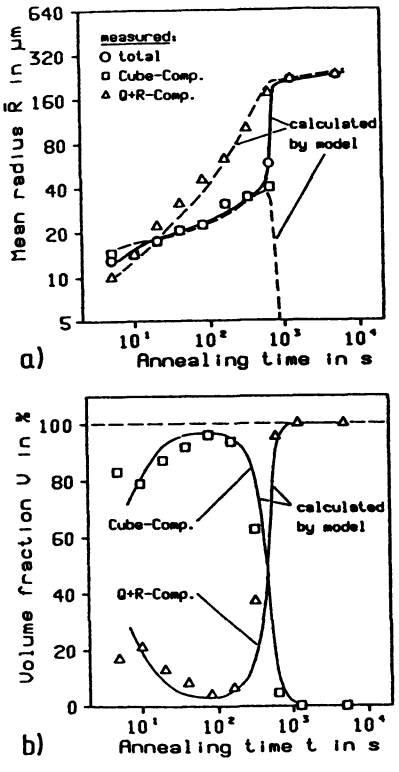

Fig.4: Comparison of experimental and model data as function of annealing time for Al 3% Mg (series I). (a) Total mean radius and partial mean radii of texture components; (b) Volume fractions of texture components.

DISCUSSION

Anisotropic energies and mobilities have two different effects on the GG kinetics which shall now be discussed. One has to recognize that the B grains, due to their lower initial frequency, are surrounded mainly by A grains thus forming A-B boundaries with high energies and mobilities. The A grains in contrast, due to their higher initial frequency, are surrounded mainly by low angle GBs with low energies and mobilities.

Let us first consider only the effect of different mobilities by assuming the GB energies to be constant. Then, due to their high mobility, at the beginning of GG small B grains will disappear and large B grains will grow very fast so that the mean grain size of B grains increases rapidly. As a consequence, in the inbetween stage of GG, few large B grains will be

embedded in a fine grained A matrix (feature of abnormal GG). Finally, B grains will occupy most of the volume, i.e. the texture changes completely.

Now let us consider only the anisotropy of GB energies by assuming the mobilities to be constant. Then the energy of the GBs surrounding B grains (A-B) is larger than of their radial (mostly A-A) GBs so that - assuming equilibrium at the GB triple points - the boundaries of B grains are curved more convexly than in the case of isotropic γ (see Figs.5a,b). Thus for B grains the critical number of sides as well as the critical radius are shifted to higher values and their probability to shrink is increased compared to the case of constant γ. This may cause an initial decrease of the volume fraction of B grains.

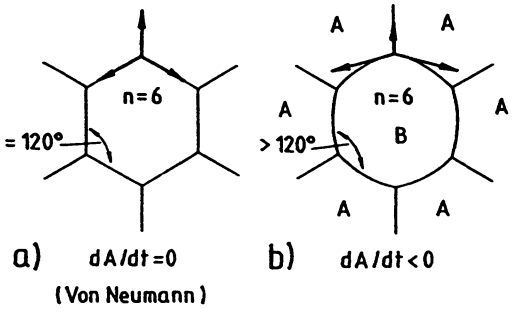

Fig.5: Growth rate (a) for a grain in a microstructure with isotropic GB energies and (b) for a grain of the minority texture component in the anisotropic energy case.

Both effects caused by the anisotropy of GBs are predicted by the AL-model. The comparison with experiments shows that it yields even a quantitative description of texture controlled GG.

ACKNOWLEDGEMENT

The authors like to thank Dipl.-Ing. S. Brodesser for supplying some experimental results. They grateful acknowledge the financial support by the Deutsche Forschungsgemeinschaft.

REFERENCES

1. J.E. Burke, *Trans. of AIME*, **180**, 73 (1949)
2. P.A. Beck, *Phil. Mag.* Supplement **3**, 245 (1954)
3. G. Abbruzzese, K. Lücke, *Acta metall.*, **34**, 905 (1986)
4. H. Eichelkraut, G. Abbruzzese, K. Lücke, *Acta metall.* **36**, 55 (1988)
5. G. Abbruzzese, K. Lücke, H. Eichelkraut, *Proc. ICOTOM 8*, (Santa Fe, 1988) p.693
6. K. Lücke, J. Pospiech, K. Virnich, J. Jura, *Acta metall.* **29**, 167 (1981)
7. W.W. Mullins, J. Appl. Phys. **27**, 900 (1956)
8. G. Abbruzzese, I. Heckelmann, K. Lücke, in press
9. X.B. Zhao, K. Lücke, to be published